

SUPPLEMENTARY INFORMATION

Characterization of Alkaline Earth Metal-doped Solid Superacid and Activity for the Esterification of Oleic Acid with Methanol

Chien-Chang Huang^{*a}, Chieh-Ju Yang^a, Pei-Jyuan Gao^a, Nai-Ci Wang^a, Ching-Lung Chen^b and Jo-Shu Chang^b

Section S1. Catalyst preparation

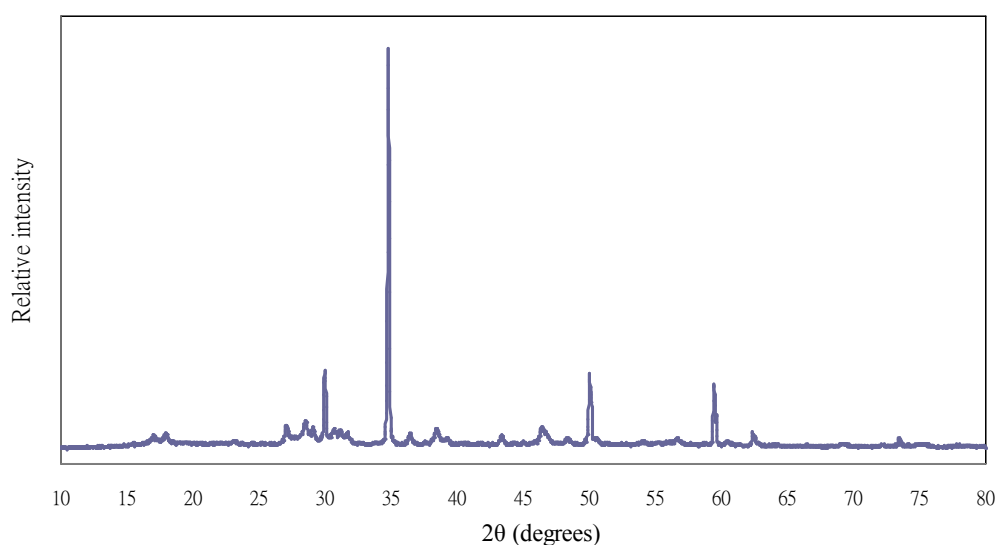


Figure S1. The XRD pattern for the sulfated strontium oxide sample. The obtained phase is indexed as SrO (JCPD No: 06-0520).

Section S2. Textural properties of the incorporated sulfate ions

The pyridine FT-IR analysis was carried out in order to study the distribution of Lewis and Brønsted acid sites on the catalysts, as well as the ratio of Lewis acid sites to Brønsted acid sites, and the corresponding spectra are shown in Figure S2. After $\text{SO}_4^{2-}/\text{Sr-Fe}$ oxide and $\text{SO}_4^{2-}/\text{Ca-Fe}$ oxide were treated with pyridine for 2 hours, and then were heated at 120°C to remove physically adsorbed pyridine in the flowing stream of N_2 , four additional adsorption bands in the region from 1440 cm^{-1} to 1620 cm^{-1} were observed (Figure S2). The shoulder band next to the band of water bending vibration at 1609 cm^{-1} and the sharp band at 1484 cm^{-1} were due to the pyridine

^a Department of Cosmetic Science, Providence University, 200 Sec. 7, Taiwan Boulevard, Shalu Dist., Taichung 433, Taiwan. Fax: +886 42631 1167; Tel: +886 42632 8001 ext. 15411; E-mail: cchuang9@pu.edu.tw

^b Department of Chemical Engineering, National Cheng Kung University, 1 University Road, Tainan 701, Taiwan. Tex: +886 6894 4496; Tel: +886 6275 7575; E-mail: changjs@mail.ncku.edu.tw

adsorbed on Lewis and Brönsted sites, respectively^{1,2}. The adsorption of pyridinium ions on Brönsted acid sites, which lead to proton transfer from the acidic hydroxyl groups (Brönsted acid sites) to adsorbed pyridine, is noted at 1530 cm⁻¹. The band at 1450 cm⁻¹ is assigned to coordinated bonded pyridine on Lewis acid sites. Therefore, the ratio of Brönsted acid sites to Lewis acid sites (N_B/N_L) can be estimated by the ratio of the integral area under the band at 1530 cm⁻¹ to that under the band at 1450 cm⁻¹. The results show that Brönsted acid sites dominate on both SO₄²⁻/Sr-Fe oxide and SO₄²⁻/Ca-Fe oxide surfaces, and SO₄²⁻/Sr-Fe oxide exhibits higher N_B/N_L (=17.5) than SO₄²⁻/Ca-Fe oxide (=15.3). In contrast, the intensity of the bands associated with the pyridine adsorbed on SO₄²⁻/Mg-Fe oxide is too low to be identified by FT-IR, indicating that only a little or none of pyridine remained on the SO₄²⁻/Mg-Fe oxide surface at 120°C. The generation of Lewis and Brönsted acid sites on sulfated alkaline earth metal-ferric oxide is due to the presence of the sulfate ions and water covalently bound to the metal cations coordinated with a sulfated ion. The surface sulfate ion has a covalent S=O bond, which also acts as an electron-withdrawing species. As sulfate ions bind to the metal cations with low electronegativity (such as Sr), the inductive effect of sulfate ions would make the metal cations become more positive (Lewis acid site). Once water molecule binds to the sulfated metal cation, the Lewis acid site is converted to Brönsted acid site via proton transfer^{3,4,5}. According to the high N_B/N_L of SO₄²⁻/Sr-Fe oxide and SO₄²⁻/Ca-Fe oxide, the model of most acid sites present on these two catalysts can be proposed.

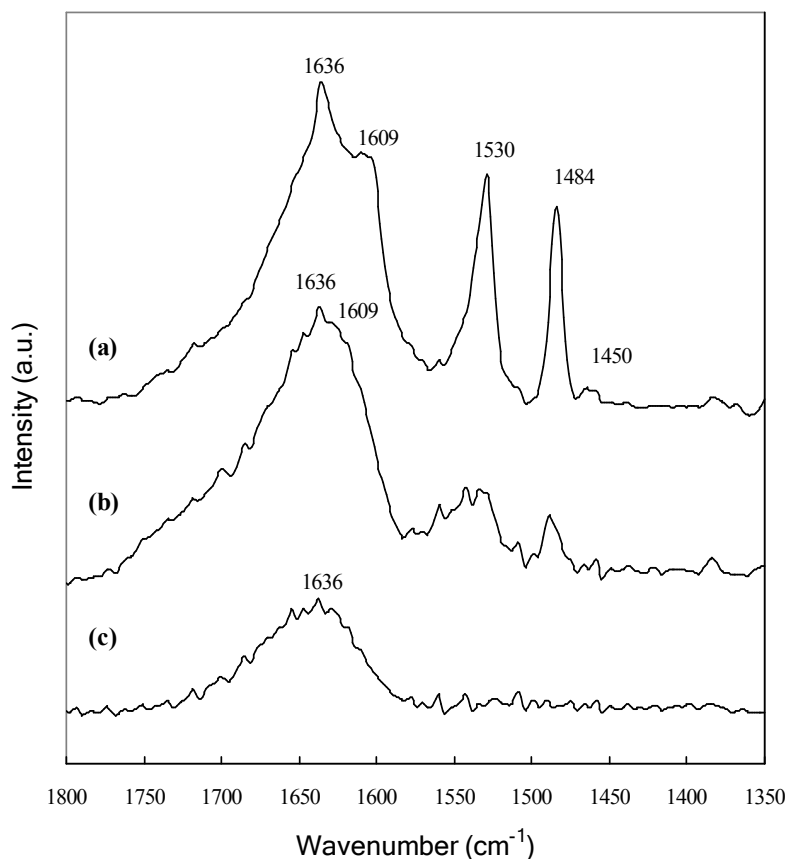


Figure S2. Correlated infrared spectra of adsorbed pyridine on (a) $\text{SO}_4^{2-}/\text{Sr-Fe}$ oxide, (b) $\text{SO}_4^{2-}/\text{Ca-Fe}$ oxide and (c) $\text{SO}_4^{2-}/\text{Mg-Fe}$ oxide

Section S3. IR studies of adsorbed oleic acid on catalyst surface

The IR spectra of the used composite oxides without sulfate modification are shown in Figure S3. As seen in Figure S3, the bands at 3015 and around 2900 cm^{-1} correspond to stretching vibrations of sp^2 -hybridized C-H and sp^3 -hybridized C-H, while the bands at 1465 and 1375 cm^{-1} are due to bending vibrations of methylene and methyl groups, respectively. The shoulder band at 1743 cm^{-1} is attributed to the C=O stretching of the COO^- moiety of a chemically adsorbed oleic acid. Another band corresponding to C=O stretching, at 1713 cm^{-1} , is also observed in the spectra due to the presence of physical adsorbed oleic acid on the most outer layer, as shown in Figure S4. Originally, the composite oxide surfaces are dominated by hydroxyl groups (the IR spectra are not shown), which exhibit a broad band in the region of 3700 to 2800 cm^{-1} , and the outermost layer is constructed by physically adsorbed water, which shows a characteristic band at 1636 cm^{-1} . After the reaction, the characteristic IR bands associated with H_2O and surface hydroxyl groups are no more

found in their IR spectra, indicating that adsorbed oleic acid completely displaces surface hydroxyl groups as the main species adsorbed on the composite oxides. It can thus be assumed that the weak broad band centered at 3463 cm^{-1} is mainly contributed by the stretching vibration of the hydrogen-bonded hydroxyl moiety of the oleic acids physically adsorbed on the most outer layer of composite oxide surface.

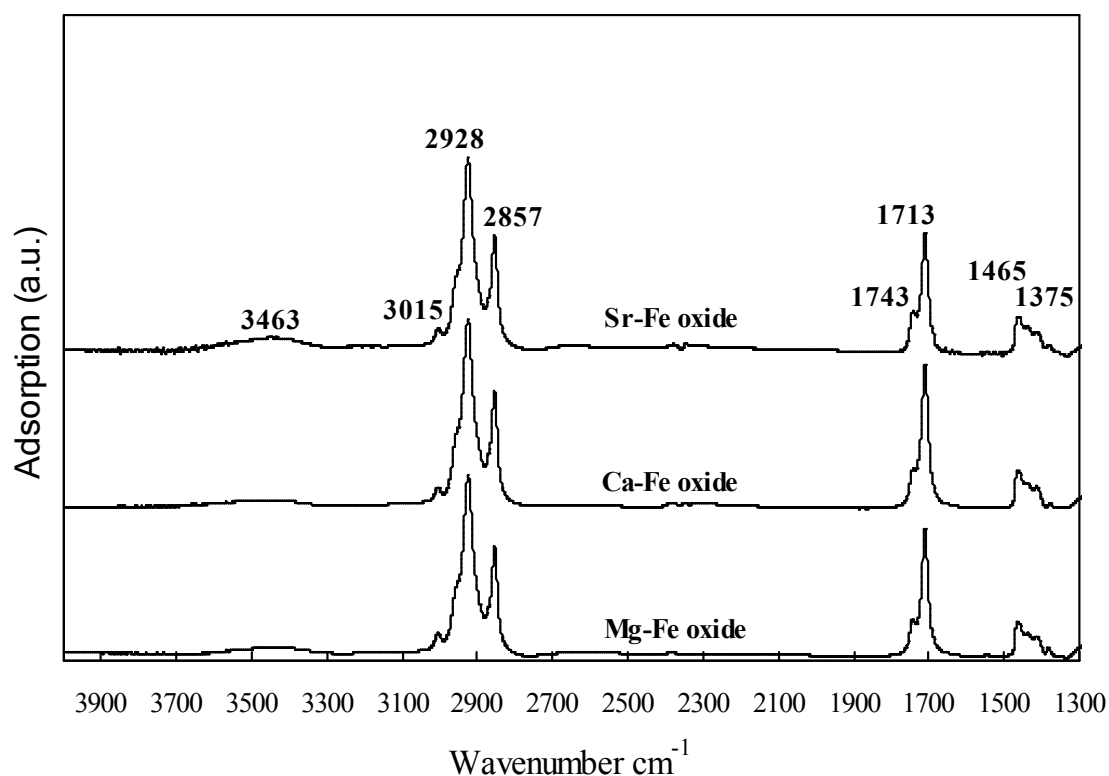


Figure S3. IR spectra of the composite oxides filtrated from the reaction mixture of oleic acid and methanol

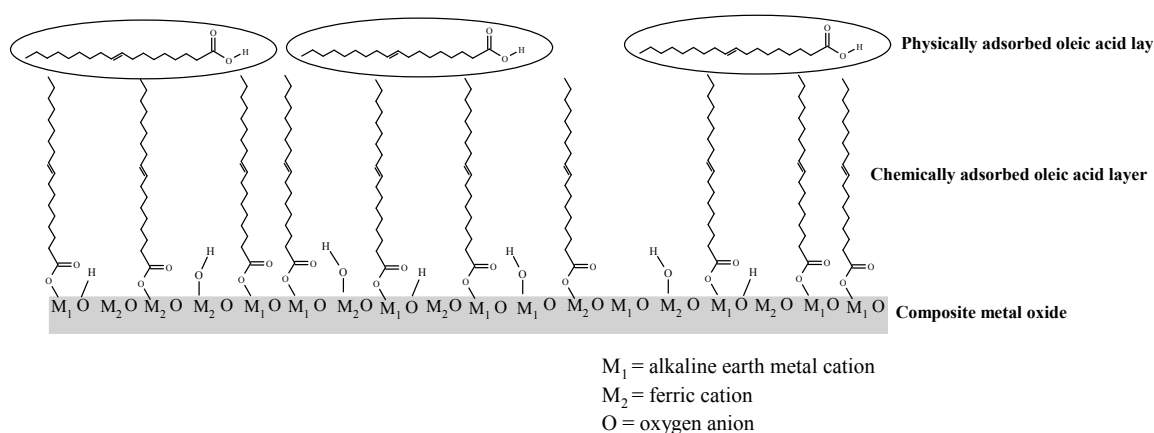


Figure S4. Proposed surface configuration of the composite oxide filtrated from the reaction mixture composed of oleic acid and methanol.

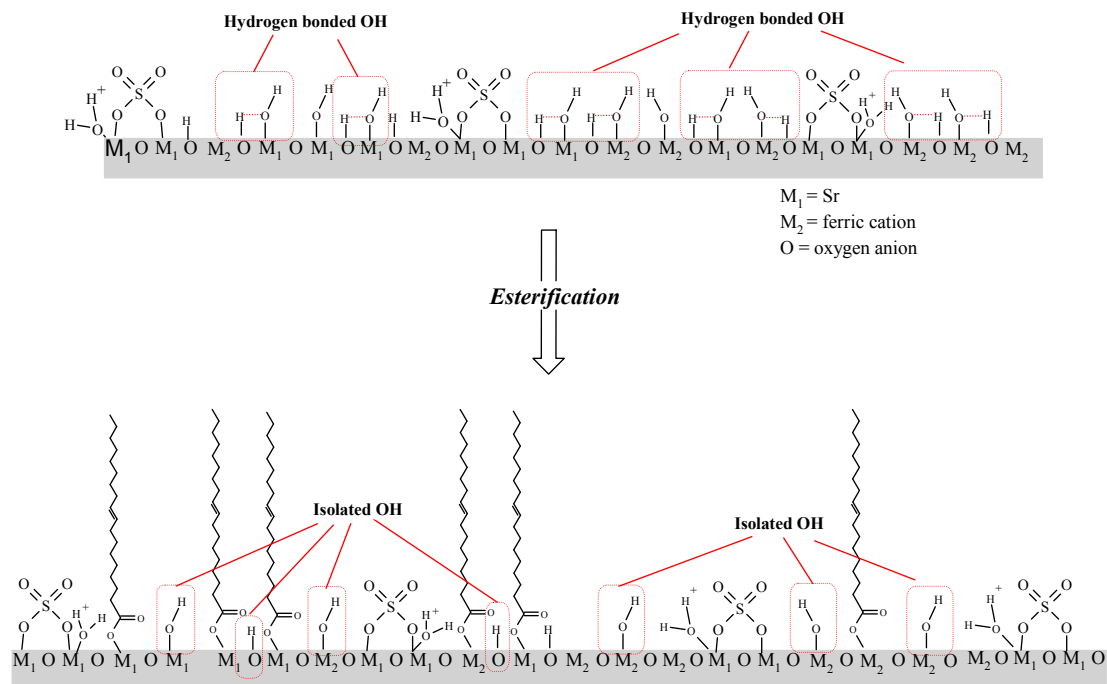


Figure S5. Schematic diagram for demonstrating the change in the configuration of surface hydroxyl groups after oleic acids binding to catalyst surface.

Section S5. Effect of the implanted iron cations on $\text{SO}_4^{2-}/\text{Sr-Fe}$ oxide reactivity

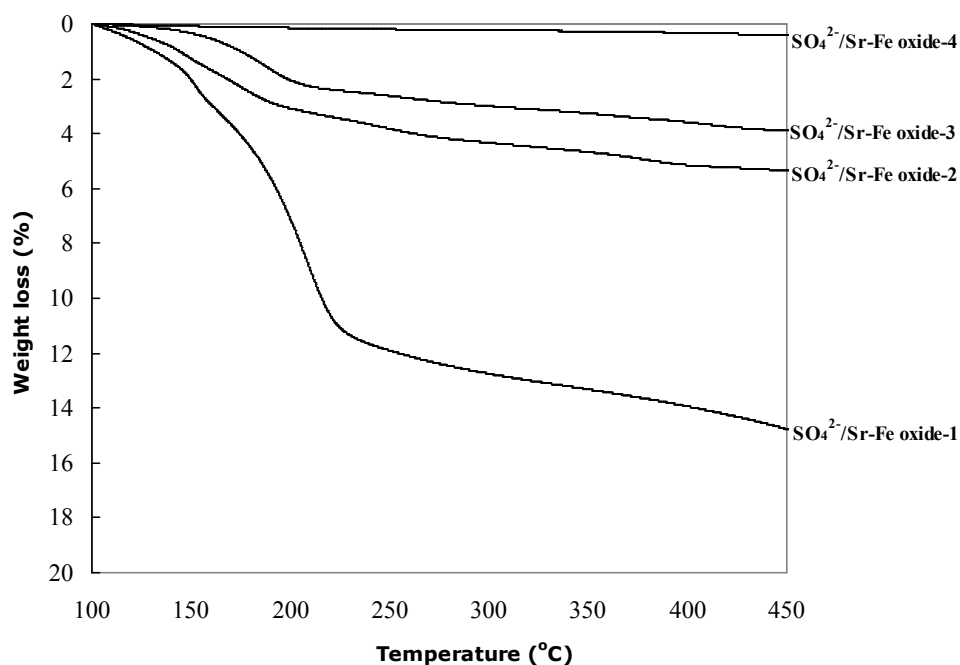


Figure S6. TGA profiles in air of the used $\text{SO}_4^{2-}/\text{Sr-Fe}$ oxide samples filtered out from the reaction mixture of the esterification after 2 hours of the reaction.

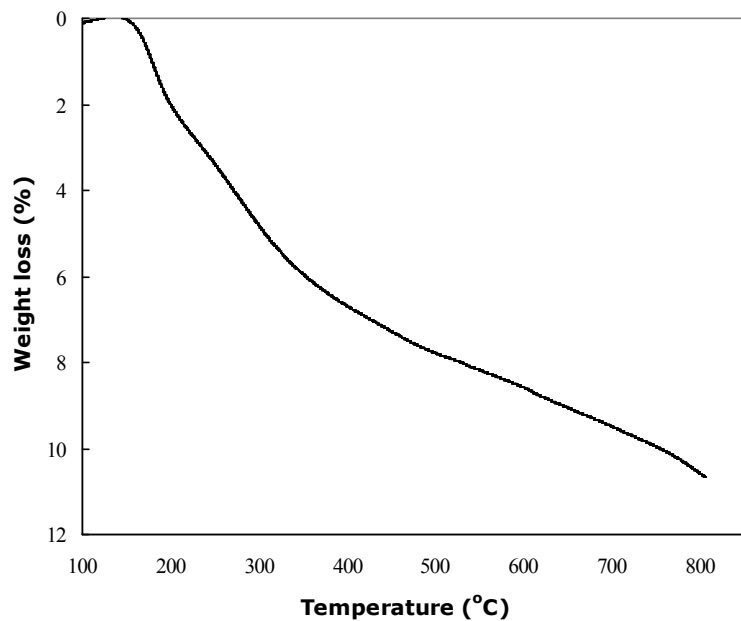


Figure S7. TGA profile in air of the used $\text{SO}_4^{2-}/\text{SrO}$.

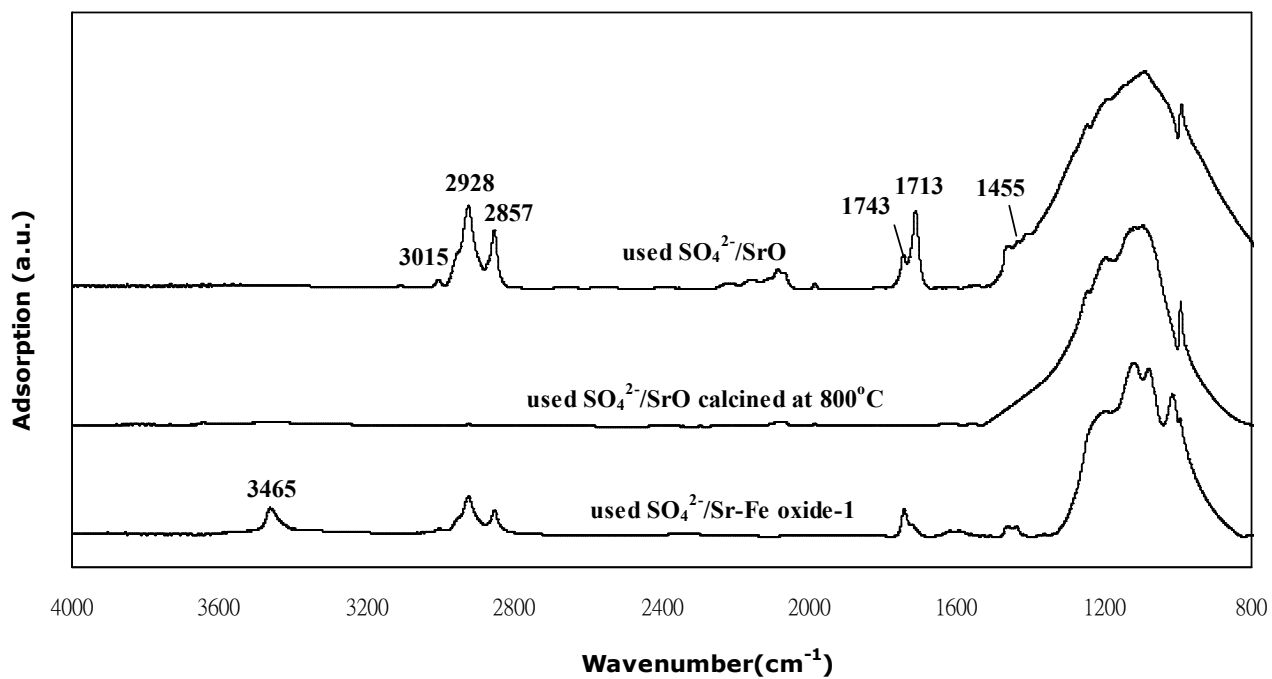


Figure S8. IR spectra of used $\text{SO}_4^{2-}/\text{Sr-Fe oxide-1}$, used $\text{SO}_4^{2-}/\text{SrO}$ and the used $\text{SO}_4^{2-}/\text{SrO}$ calcined at 800°C for 2 hours.

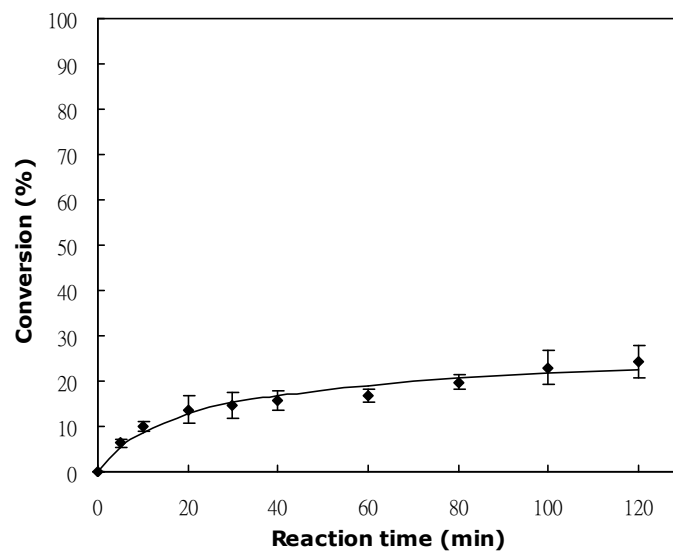


Figure S9. Conversion versus reaction time for the oleic acid esterification catalyzed by $\text{SO}_4^{2-}/\text{SrO}$ at 100°C .

Section 6. Kinetic study

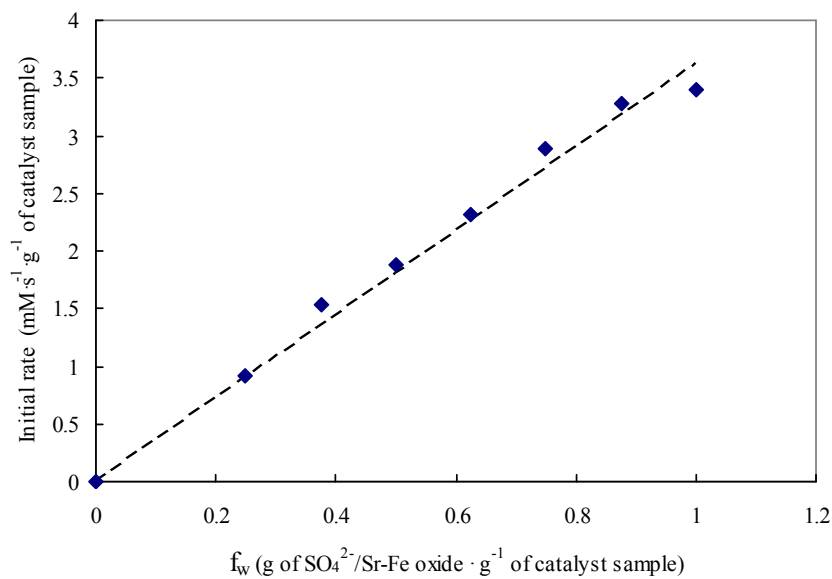


Figure S10. The initial rates of the esterification per gram of the catalyst samples consisting of $\text{SO}_4^{2-}/\text{Sr-Fe}$ oxide and inert powder, SiO_2 , at 100°C . The weight fraction (f_w) of $\text{SO}_4^{2-}/\text{Sr-Fe}$ oxide in the catalyst samples was varied from 1 to 0.25.

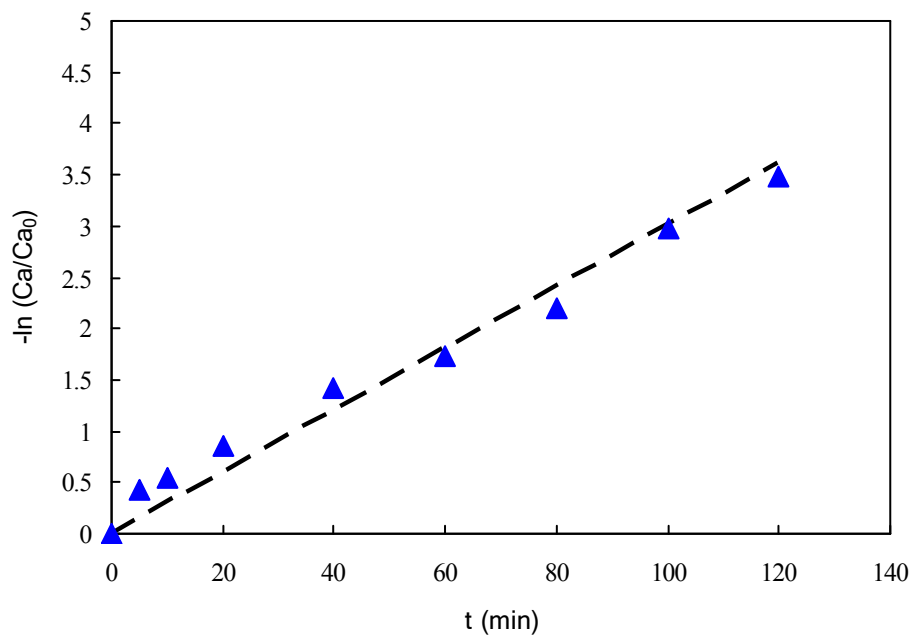


Figure S11. First order rate equation fitting the data of the esterification of oleic acid with methanol (molar ratio 1:4) over $\text{SO}_4^{2-}/\text{Sr-Fe}$ oxide at 100°C .

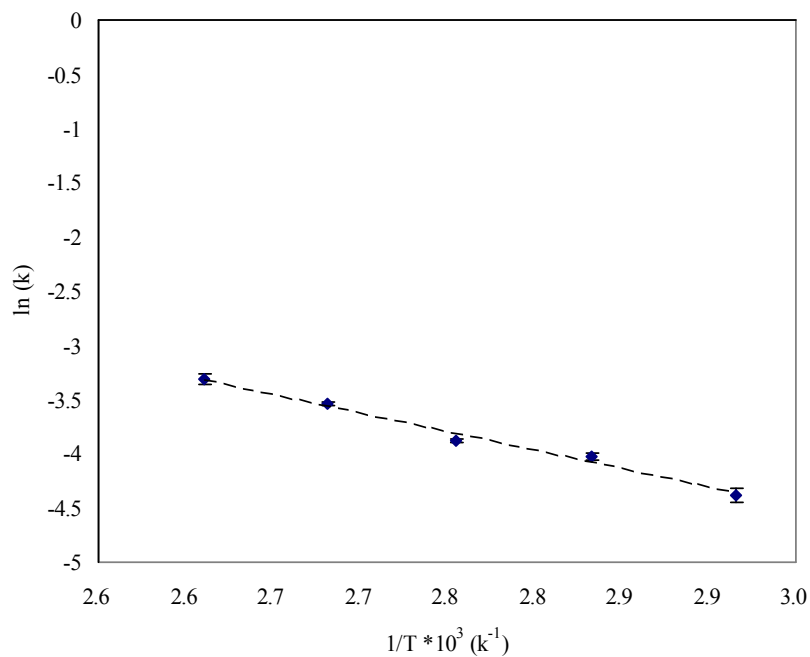


Figure S12. Arrhenius plot ($\ln(k)$ versus $1/T$) to determine the activation energy.

Table S1. Kinetic parameters for the catalyzed esterification of fatty acids with short chain alcohols

Catalyst	Reaction conditions ^a	FFA conversion	R ^b (mMs ⁻¹ g ⁻¹)	Rate constant (×10 ³ min ⁻¹)	TOF (min ⁻¹)	Ref.
Sulfated zirconia	Myristic acid+methanol, MR=1:10, T=60°C, t=420 min, Cat.= 0.5 wt%.	>98%	n.a.	18.79	0.074	6
Sulfated zirconia incorporated on SBA-15	Palmitic acid+methanol, MR=1:88, T=68°C, t=360 min, Cat.= 20 wt%.	89%	0.04	7.03	0.14	7
Sulfated titania	Oleic acid+ethanol, MR=1:10, T=80°C, t=180 min, Cat.=2wt%	82%	4.89	10.46	0.67	8
Sulfated zirconia	Oleic acid+methanol ^c , MR=1:33, T=60°C, t=80 min, Cat.=2wt%	83%	0.28	23.60	n.a.	9
Sulfated zirconia	Oleic acid+methanol, MR=1:10, T=100°C, t= 300 min, Cat.=3wt%	98%	1.07	4.6	1.70	10
Sulfated zirconia/metal organic framework	Oleic acid+methanol, MR=1:77, T=100°C, t= 600 min, Cat.=11wt%	98%	0.04	4.55	0.26	11
Present work SO ₄ ²⁻ /Sr-Fe oxide	Oleic acid+methanol, MR=1:4, T=100°C, t=120 min, Cat.=10wt%	98%	3.44	29.68	1.06	-

^a MR=molar ratio of FFA to alcohol, t=reaction time, T=reaction temperature, Cat.=Catalyst loading referred to FFA weight.

^b R=initial reaction rate

^c the conversion of the oleic acid mixed in soybean oil. The volume percentage of oleic acid in soybean oil is 10%.

References

- 1 A. Mantilla, G. Ferrat, A. López-Ortega, E. Romero, F. Tzompantzi, M. Torres, E. Ortíz-Islas, R. Gómez, *J. Mol. Catal. A*, 2005, **228**, 333.
- 2 M. Álvarez, M.J. Ortiz, J.L. Roper, M.E. Niño, R. Rayon, F. Tzompantzi, R. Gomez, *Chem. Eng. Comm.*, 2009, **196**, 1152.
- 3 H. Ahn, C.P. Nicholas, T.J. Marks, *Organometallics*, 2002, **21**, 1788.
- 4 V. Adeeva, J.W. de Haan, J. Jänchen, G.D. Lei, V. Schünemann, L.J.M. van de Ven, W.M.H. Sachtler, R.A. van Santen, *J. Catal.*, 1995, **151**, 364.
- 5 S. Wang, S. Matsumura, K. Toshima, *Tetrahedron Lett.*, 2007, **48**, 6449.

-
- ⁶ K. Saravanan, B. Tyagi, C. Bajaj, *Catal. Sci. Technol.*, 2012, **2**, 2512.
- ⁷ X.-R. Chen, Y.-H. Ju, C.-Y. Mou, *J. Phys. Chem. C*, 2007, **111**, 18731.
- ⁸ J.L. Roperov-Vega, A. Aldana-Pérez, R. Gómez, M.E. Niño-Gómez, *Appl. Catal. A*, 2010, **379**, 24.
- ⁹ V.G. Deshmane, Y.G. Adewuyi, *Appl. Catal. A*, 2013, **462-463**, 196.
- ¹⁰ J.K. Satyarthi, D. Srinivas, P. Ratnasamy, *Energy Fuels*, 2010, **24**, 2154.
- ¹¹ E.Y. Park, Z. Hasan, I. Ahmed, S.H. Jung, *Bull. Korean Chem. Soc.*, 2014, **35**, 1659.